SMGroup

SM Journal of Biology

Research Article

Distribution of Acetylated Histone 4 in Normal Liver and Acetaminophen-Induced Liver Damage

Nakamura N[1]*, Chang C-W[2], Yang X[1], Shi Q[1], Salminen WF[1] and Suzuki A[3,4]

[1]*Division of Systems Biology, National Center for Toxicological Research, Food and Drug Administration, United States*

[2]*Division of Bioinformatics and Biostatistics, National Center for Toxicological Research, Food and Drug Administration, United States*

[3]*Division of Gastroenterology, Central Arkansas Veterans Healthcare System, United States*

[4]*Division of Gastroenterology, University of Arkansas for Medical Sciences, United States*

Article Information

Received date: Dec 23, 2016
Accepted date: Feb 01, 2017
Published date: Feb 06, 2017

***Corresponding author**

Nakamura N, Division of Systems Biology, National Center for Toxicological Research, Food and Drug Administration, United States, Tel: +1-870-543-7175; Fax: +1-870-543-7662; Email: Noriko.Nakamura@fda.hhs.gov

Keywords Acetaminophen; Liver; Mice; Necrosis; Histone acetylation

Abstract

To describe cell-specific acetylation of histones and their zonal localization in normal mouse liver and characterize their changes in acetaminophen (APAP)-damaged mouse liver 24 hr after APAP exposure, we performed an immunohistochemical study using normal and APAP-injured mouse livers. Cell-specific expression of acetylated H4 was observed in normal mouse liver. The highest acetylated H4 expression levels were found in bile duct epithelial cells, followed by sinusoidal non-parenchymal cells, venous endothelial cells, and hepatocytes. Zonal differences were observed; acetylated H4 expression was stronger in zone 1 (periportal) than in zone 3 (pericentral). In APAP-treated mouse liver, acetylated H4 expression decreased as tissue damage developed, and was significantly negatively correlated with tissue damage and alanine aminotransferase levels ($p<0.05$). Acetylated H4 expression in sinusoidal non-parenchymal cells did not decrease after tissue damage. The method implemented herein can measure acetylated H4 expression in a cell- and zone-specific manner and aid future investigation on pathobiological relevance of altered histone modification in liver injury and repair.

Introduction

Epigenetic modifications (e.g., DNA methylation and post-transcriptional histone protein modification) regulate gene expression and influence cellular functions and phenotypes without changing the DNA sequence [1,2]. Histone acetylation facilitates the binding of chromatin to transcription factors that promote gene expression. These alterations are dynamic and responsive to environmental stimuli throughout life and can interface between environmental factors and pathological processes. To date, epigenetic changes have been associated with a range of diseases, including cancers, autoimmune conditions, and cardiovascular disease, as well as the aging process [4-7].

Modifications of histone acetylation are known to delay liver regeneration after acute assault in mice and humans [8,9]. Thus, they are likely to have significant roles in hepatic tissue injury and repair. However, the mechanism by which altered histone acetylation contributes to liver injury and/or repair has not been fully understood. Most previous studies have analyzed either gene or protein expression of acetylated histones using homogenized liver tissues, but no studies have investigated the degree and localization of histone acetylation in normal and injured livers. To better understand the pathobiological significance of epigenetic modifications in the liver, it is critical to characterize cell-specific epigenetic profiles (parenchymal *vs.* non-parenchymal cells) and zonal localization [10] in normal liver architecture, and to characterize the changes of epigenetic parameters during the course of liver injury relative to tissue damage. Developing a tool for measuring the profile of epigenetic modification in the liver is necessary for such investigations in future.

In this study, we performed immunohistochemical evaluations of histone acetylation (H4) in normal liver and acetaminophen (APAP)-induced liver injury. We chose the APAP-induced liver injury model that was used in a previous study [11] because it is a well-established liver injury model and it's injury pattern and mechanisms have been well characterized [12-14]. Our aims were to (1) describe cell-specific histone acetylation and zonal localization in normal liver tissues, and (2) characterize the changes in cell-specific histone acetylation and zonal distribution in APAP-injured mouse livers that occur up to 24 hr after APAP exposure. Our goal was to implement methodology to investigate cell-/zone-specific epigenetic modifications during liver injury and their relationship to degree of tissue repair and overall outcomes in future studies.

Table 1: Scoring of for necrotic tissue damage in APAP-exposed mouse liver (modified Derelanko, 2008).

Numerical Score	Description	Frequency
0	Normal	< 1%
1	minimal	1-25%
2	mild	26-50%
3	moderate	51-75%
4	marked including bridging	75-100%

Materials and Methods

Materials

All reagents were purchased from Fisher Scientific (Pittsburgh, PA, USA), unless otherwise indicated.

Animals and treatments

Male B6C3F1/Nctr mice (6- to 7-week-old) were obtained from a breeding colony at the National Center for Toxicological Research (NCTR). Animals were housed individually and maintained under a 12-h light-dark cycle at controlled room temperature (23 °C ± 3 °C) and humidity (50% ± 20%). Water was provided *ad libitum*. All animal procedures were approved by the NCTR Institutional Animal Care and Use Committee and followed the guidelines set forth by the National Research Council Guide for the Care and Use of Laboratory Animals [15]. The principles of laboratory animal care outlined in NIH publication No. 86-23 (revised 1985) were followed.

The animals were treated with APAP as previously described by Yang, et al [11]. In brief, they were fasted overnight and then administered either 300 mg/kg APAP (Sigma-Aldrich, St. Louis, MO, USA) in 0.5% methylcellulose or 0.5% methylcellulose (control group) by oral gavage. Animals (n=3–5) were sacrificed and their livers were collected after 1, 3, 6, and 24 hr. To determine the normal distribution of acetylated H4, mice were dosed with 0.9% saline by intraperitoneal injection (normal mice) (n=3). Liver tissues were collected from the mice and fixed with 10% formalin for approximately 48 hr for histological analyses, followed by embedding in paraffin for subsequent sectioning.

Necrotic tissue damage evaluation

To evaluate tissue damage, we performed Hematoxylin and Eosin (H&E) and terminal deoxynucleotidyl transferase-mediated deoxyuridine triphosphate nick-end labeling (TUNEL) staining [16]. Paraffin blocks were prepared using standard procedures and 5-μm liver sections were cut. After deparaffinization, slides were stained with hematoxylin QS (Vector Laboratories, Burlingame, CA, USA) for 30 sec, washed in running water, and stained with 1% eosin/alcohol solution (Sigma-Aldrich) for 2 min. The stained slides were dehydrated and mounted with Poly-Mount (Polysciences Inc., Warrington, PA, USA). Images were captured with a Zeiss microscope and AxioVision software (Carl Zeiss Microscopy, LLC, Thornwood, NY, USA) using the same exposure time for all images.

TUNEL staining was performed using an *in situ* cell death detection kit (Roche Diagnostics, Corp., Indianapolis, IN, USA) according to the manufacturer's instructions. In brief, liver sections were treated with 10μg/mL proteinase K in phosphate-buffered saline at 37 °C for 30 min, then washed with phosphate-buffered saline, and incubated with TUNEL reaction mixture at 37 °C for 60 min. The sections were then washed with phosphate-buffered saline and counterstained with 1 μg/mL propidium iodide (MP Biomedicals, Santa Ana, CA, USA). Images of the TUNEL-stained sections were recorded with a Zeiss microscope and AxioVision software (Carl Zeiss Microscopy) using the same exposure time. The severity of hepatocyte necrosis was quantified as described by Derelanko [17], with a minor modification (i.e., necrosis score; Table 1).

Immunofluorescent staining

Immunofluorescence studies were performed as described by Wade, et al. [18], with few modifications. Antibodies to acetylated histone H4 (cat#: 06-866, rabbit polyclonal) were purchased from Millipore (Temecula, CA, USA). Liver sections were deparaffinized and incubated with 1 mM Ethylenediaminetetraacetic Acid (EDTA; pH 8.0) in 0.05% Triton X-100 diluted with distilled water at 95-100 °C for 45 min. The sections were then cooled for 20 min at room temperature prior to blocking with Tris-buffered saline containing 0.002% Triton X-100 (TBST), with 1% Bovine Serum Albumin (BSA) and 5% goat serum (Vector Laboratories) for 20 min at room temperature. The sections were then incubated at 4 °C overnight with primary antibodies (anti-acetylated histone H4 [1:250 dilution]) diluted in TBST with 1% BSA. Negative controls were similarly prepared with no primary antibodies. After washing three times with TBST, each section was incubated with Alexa Fluor 594 goat anti-rabbit IgG antibody (1:100 dilution; cat#: A-11012; Life Technologies, Carlsbad, CA, USA). The stained slides were mounted with ProLong Gold Antifade Mountant with 4',6-Diamidino-2-Phenylindole (DAPI; Life Technologies). The images were then captured with a Zeiss microscope and AxioVision software (Carl Zeiss Microscopy, LLC) or Nikon ECLIPSE E400 (Nikon instruments Inc., Melville, NY, USA) and NIS element-viewer software (Nikon instruments Inc.). Although immunohistochemistry with diaminobenzidine detection found overall expression of acetylated H4 in mouse liver, differences in cell-specific expression levels could not be fully discerned. We chose to employ immunofluorescent staining in this study, as it was more suitable for investigating degrees of cell- or zone-specific expression.

Quantitative image analysis of liver sections

For acetylated H4 and TUNEL stains, 10 randomly selected fields of acetylated H4 and TUNEL-stained liver sections were captured using a Zeiss microscope (×20 objective lens) and AxioVision software version 4.8.2 (Carl Zeiss Microscopy, LLC) [19]. Positive cells were then counted in each field by the AxioVision software and expressed as the average number of positive cells per field.

The zonal intensity (periportal *vs.* pericentral area) of acetylated H4 staining was analyzed using a Zeiss microscope and AxioVision software version 4.8.2 (Carl Zeiss Microscopy, LLC). More specifically, the zonal intensity of acetylated H4 staining was measured in hepatocytes located within three to four cell layers from the portal vein (periportal area) and central vein (pericentral area), while excluding signals from endothelial cells of the portal and central veins as well as bile duct cells (Supplemental Figure 1a, b). The above measurement was performed on entire liver sections per animal. Mean intensities in the periportal and pericentral areas were calculated in individual

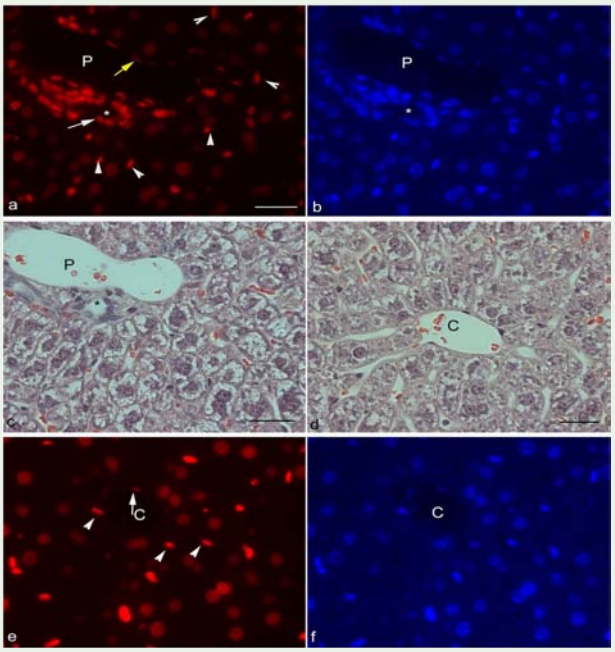

Figure 1: Expression of acetylated H4 in normal mouse liver.
Mouse liver sections were incubated with acetylated H4 antibody (a, c). DAPI was used for nuclei staining (e, f). The images were observed at ×60 magnification (a, b, e, and f). The serial sections were stained with H & E and these images were observed at ×40 magnification (c, d). (a, b, c) show the periportal area, while (d, e, f) show the pericentral area. Acetylated H4 was strongly expressed in bile duct epithelial cells (a; arrows) and sinusoidal non-parenchymal cells (arrowheads) in the lobules of mouse liver sections. In contrast, hepatocytes were weakly stained by acetylated H4 antibodies. Acetylated H4 was strongly expressed in endothelial cells in the veins (c; arrows). In contrast, hepatocytes were weakly stained by acetylated H4 antibody. P: portal vein; C: central vein; *: bile ducts. Bars: 20 μm.

animals. The difference in zonal intensity of acetylated H4 staining was calculated by subtracting the mean intensity of staining in the pericentral area from that of the periportal area for each animal by Microsoft Excel software (Microsoft, Redmond, WA, USA). And then, we calculated means and standard deviations of the difference in zonal intensity each group at different time points.

Statistics

Statistical analyses were performed using Student's *t*-tests or one sample *t*-tests. The values are presented as the mean ± standard deviation, and the significance level was fixed at $p < 0.05$. Multiple linear regression analysis was also performed, including H4 staining or necrotic scores or serum alanine aminotransferase (ALT) as an outcome, and time (hr) after exposure to APAP as a covariate (included as an ordinal variable). The partial correlation coefficient was calculated using a regression model to assess the relationship between H4 staining and ALT or necrotic scores after adjusting for time-dependent differences. Image data processing and statistical analyses were performed using Microsoft Excel 2007, GraphPad Prism version 6 (GraphPad, La Jolla, CA, USA), and R [20].

Results and Discussion

Localization and intensity of acetylated H4 in normal mouse liver

Both bile duct epithelial cells and hepatocytes were stained by acetylated H4 antibody (Figure 1a). Bile duct epithelial cells were strongly positive for acetylated H4 and generally showed stronger staining than hepatocytes (Figure 1a; arrow). Acetylated H4 expression in the endothelial cells of portal vein was slightly weaker than ones in the bile duct epithelial cells (Figure 1a; yellow arrow). Overall, there was a zonal difference in the intensity of acetylated H4 expression in hepatocytes: expression in the periportal area was consistently stronger than that in the pericentral area in all normal mice (average difference with standard deviation: 24.52±12.26; p=0.074, n=3; one sample *t*-test). Sinusoidal non-parenchymal cells, which were differentiated from hepatocytes based on the size and form of their nuclei (Figure 1a, c; arrowheads), and endothelial cells of central veins (Figure 1c; arrow) expressed a higher level of acetylated H4 than hepatocytes. No signals were detected in the negative controls (without primary antibodies; Figure Supplemental 2a, b).

In summary, acetylated H4 exhibited zone- and/or cell-specific expression patterns in normal mouse livers, with the highest intensity of acetylated H4 staining observed in bile duct epithelial cells, followed by sinusoidal non-parenchymal cells, venous endothelial cells, and hepatocytes (Table 2). Zonal differences in acetylated H4 staining were observed among hepatocytes, with stronger expression in zone 1 (periportal) versus zone 3 (pericentral). A few published studies using immunofluorescence found that acetylated histones were expressed in neoplastic human tissues paired with adjacent non-neoplastic tissues or cultured cell lines. Others reported the expression of acetylated H4 in a human adenocarcinomic alveolar epithelial cell line (A549) and human tissues: gastric cancer, gastric adenoma, and non-neoplastic tissues adjacent to gastric tumors (nuclei of epithelial and stromal cells) [21,22]. However, no studies have used normal liver tissues to address the cell- and zone-specific expression patterns of acetylated H4. Our immunohistochemical evaluation revealed an interesting zonal difference in fluorescence intensity of acetylated H4, which was consistently stronger in the periportal area than the pericentral area. The function of hepatocytes in each zone is known to differ for glucose metabolism, ammonia detoxification, and other processes [23,24]. Theise, et al. [25] reported that hepatic stem cells in humans were thought to be in the "Canals of Hering" in the bile duct and new hepatocytes were produced continuously in the portal vein (zone 1) and moved toward the central vein (zone 3). This observation may reflect more active transcriptional activity in zone 1, where higher numbers of hepatocytes are generated by stem cells compared to zone 3 [26]. The cell-specific expression of acetylated histone protein, H4 suggest different biophysiological roles in normal livers, but further investigation is necessary.

Localization and intensity of acetylated H4 in APAP-induced injured mouse liver

Hepatocyte necrosis induced by APAP: Liver sections from mice treated with APAP and controls were analyzed for degrees of

Table 2: Staining of acetylated H4 in normal mouse liver.

	Hepatocytes	Ductal cells (bile duct)	Sinusoidal Non-parenchymal cells	Endothelial cells in vein
Acetylated H4	+	+++	++	+~++ (P, C)

P=portal vein; C=central vein. Immunohistochemistry were categorized into five levels: -, no detection; ±, faint; +, weak; ++, moderate; +++, strong.

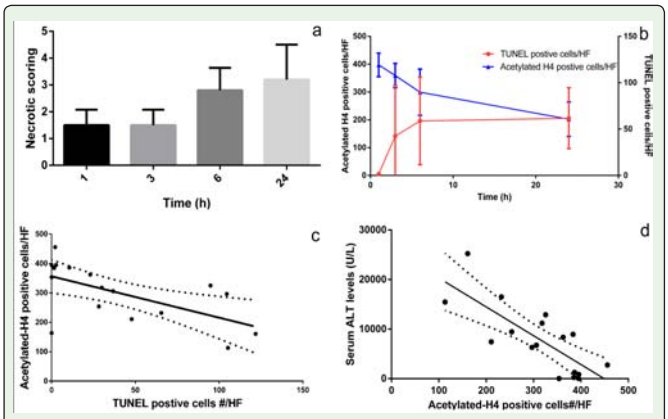

Figure 2: Semi-quantitative analysis of acetylated H4 levels in APAP-treated mice.
The graph shows the necrotic tissue damage scoring at 1, 3, 6, and 24 hr. Data are expressed as mean ± standard deviation, n=3–5. (b) The numbers of acetylated H4-positive cells/High Magnification Field (HF) are shown on the left y-axis and the numbers of TUNEL-positive cells (necrosis)/HF are shown on the right y-axis at 1, 3, 6, and 24 hr. Data are expressed as mean ± standard deviation, n=3–5. (c) Correlation between TUNEL-positive cell number/HF and acetylated H4-positive cell number/HF. Dotted lines represent 95% confidence intervals. (d) Correlation between serum ALT levels and acetylated H4-positive cell number/HF. Dotted lines represent 95% confidence intervals.

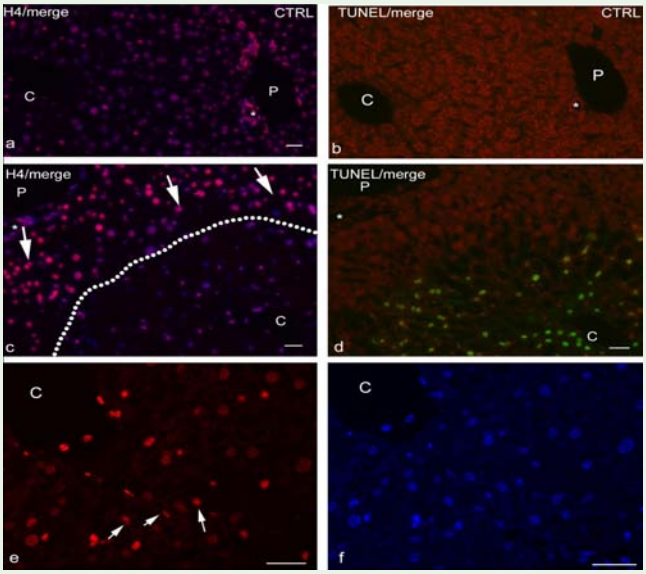

Figure 3: Liver expression of acetylated H4 in APAP-treated mice at 3 hr after APAP administration.
Liver sections from control (a, b) and APAP-treated (c, d) mice at 3 hr were reacted with acetylated H4 antibody or stained with TUNEL. The images were observed at ×40 magnification (a-d). (a, c) show the merged images of acetylated H4/DAPI (blue) shown in pink. (b, d) show the merged TUNEL/propidium iodide (PI)-stained images of each group; TUNEL-positive cells (green), PI (red), and merged images (yellow). White dotted line shows the border of necrosis area (c). (e, f) show the pericentral area with a higher magnification. Acetylated H4 was strongly expressed in sinusoidal non-parenchymal cells (a; arrows). The images were observed at x60 magnification (e, f) (e) shows the image of immunostaining with acetylated H4 antibody. DAPI was used for nuclei staining (f). P: portal vein; C: central vein; *: bile ducts. Bars: 50 μm.

hepatocyte necrosis (necrotic scores) up to 24 hr after APAP exposure by using H&E and TUNEL. Necrotic scores by H&E and TUNEL in APAP-treated mice significantly increased 1, 3, 6, and 24 hr after APAP exposure (Figue 2a, b: red line).

Changes in acetylated H4 staining in response to tissue damage: Liver sections from mice treated with APAP and controls were analyzed for acetylated H4 using immunohistochemistry to assess changes over time, which we used to correlate with degree of tissue damage (i.e., hepatocyte necrosis) following APAP exposure. No significant changes were observed in the acetylated H4-stained tissue at 1 hr after APAP exposure (Supplemental Figure 3). At 3 hr after APAP exposure, the number of acetylated H4-positive hepatocytes significantly decreased in the pericentral area of APAP-treated mice (Figure 3c), where strong TUNEL staining (necrotic area) was observed compared to that of control mice (Figure 3d). In a periporal area adjacent to the necrotic area (Figure 3c, dotted line) where no necrosis was observed, acetylated H4 signals in hepatocytes appeared to be increased (Figure 3c, arrows) compared to the control (Figure 3a). At 24 hr, acetylated H4-negative hepatocytes were observed in periportal area where showed TUNEL-positive staining (Figure 4a; arrows, blue color). Acetylated H4 expression in bile duct epithelial cells and endothelial cells of the portal vein did not show any apparent changes up to 24 hr after APAP exposure (Figure 4a, pink color). No changes in acetylated H4 expression in hepatocytes, non-parenchymal cells (Figure 3e, arrows), bile duct epithelial cells, and portal and central vein endothelial cells were observed in the control mice at any of the time points examined (Figure 3a and Supplemental Figure 3). Acetylated H4-positive cells were decreased at 1, 3, 6 and 24 hours after APAP exposure (Figure 2b; blue line).

Overall, there was a negative correlation between the intensity of TUNEL staining and the number of acetylated H4-positive cells over the course of liver injury (Figure 2c). After adjusting for the effect of time, we discovered a significant negative correlation between the two signals (partial r=-0.8141, p=0.00022). In addition, using serum ALT levels from a previous study [11], a negative correlation between serum ALT levels and the number of acetylated H4-positive cells over the course of liver injury was found (Figure 2d). We found a significant negative correlation between serum ALT levels and acetylated H4-positive cells after adjusting for the effect of time (partial r=-0.45, p<0.004).

Control mice showed zonal differences in the intensity of acetylated H4 expression regardless of the time points as observed

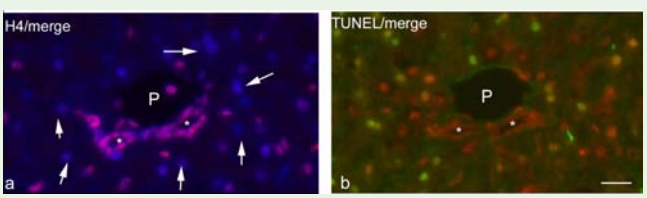

Figure 4: Liver expression of acetylated H4 in APAP-treated mice at 24 hr after APAP administration.
Liver sections from APAP-treated (a, b) mice at 24 hr were reacted with acetylated H4 antibody or stained with TUNEL. The images were observed at ×40 magnification. (a) shows the merged images of acetylated H4/DAPI (blue) shown in pink. (b) shows the merged TUNEL/propidium iodide (PI)-stained images of each group; TUNEL-positive cells (green), PI (red), and merged images (yellow). C: central vein. Bars: 50 μm.

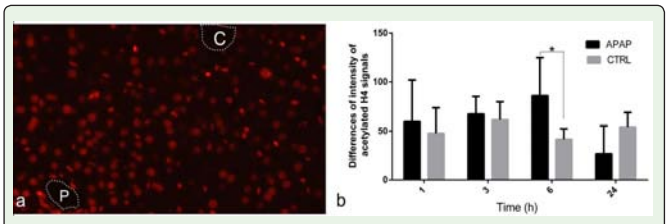

Figure 5: Zonal difference in intensity of acetylated H4 staining in APAP-treated mice.
(a) Acetylated H4 expression in the periportal and pericentral areas of control mouse liver sections. The images were observed at ×20 magnification. Veins are indicated by a dotted line. C: central vein; P: portal vein. (b) The graph shows the difference between the intensity of acetylated H4 signals in the periportal and pericentral areas in the APAP-treated groups at 1, 3, 6, and 24 hr compared to that in the control mice. The method for calculating the differences is listed in the Materials and Methods section. Data are expressed as mean ± standard deviation, n=3–5. $^{*}p < 0.05$, compared to the controls.

in the normal liver: periportal expression was consistently stronger than pericentral expression in all control mice ($p<0.05$; one sample t-test; data not shown). In contrast, the zonal difference in intensity of acetylated H4 staining in APAP-treated mice increased over the course of injury: the intensity in the pericentral area declined, but was retained in the periportal area (Figure 5b). The zonal difference in intensity was calculated for each mouse and compared with that of the APAP-treated mice and control mice. The difference between APAP-treated and control mice was greatest at 6 hr after APAP exposure, which was statistically significant (Figure 5b), although the difference did not reach statistical significance at other time points because of the small sample number and wide range of zonal differences among animals.

As summarized in Table 3, Hepatocyte staining of acetylated H4 in APAP-treated mice significantly decreased with progression of tissue damage following APAP exposure. There was a significant negative correlation between increased necrosis and decreased histone H4 acetylation. Of note, we observed some acetylated H4-negative hepatocytes in injured tissues in the periportral area at 24 hr. However, the nature of hepatocytes lacking acetylated H4 expression remains unknown. One possibility is that decreased H4 expression may likely affect gene or protein expression in the pericentral area of hepatocytes [27], resulting in arrested proliferation of damaged hepatocytes [28].

Interestingly, the expression of acetylated H4 in sinusoidal non-parenchymal cells did not change, even after tissue damage (necrosis) occurred. This finding is intriguing, as sinusoidal endothelial and satellite cells are known to regulate liver regeneration after injury [29] and induce the proliferation of hepatocytes [30]. Thus, the non-parenchymal cells may promote hepatocyte proliferation by keeping histone acetylation levels high in liver injury. Whether altering histone acetylation of sinusoidal non-parenchymal cells or hepatocytes would significantly influence regenerative activity after liver injury is unknown.

Table 3: Summary of alteration of necrotic scores, TUNEL and acetylated H4 staining in hepatocytes of APAP-exposed mouse liver.

		1 hour	3 hours	6 hours	24 hours
Necrotic scores		1.5 ± 0.6	1.5 ± 0.6	2.8 ± 0.8	3.8 ± 0.5
TUNEL	Central	-~±	+~++	++~+++	++~+++
	Portal	-	-	-	+
Acetylated H4	Central	++	++	+~++	-~+
	Portal	+++	+++	+++	++~+++

All findings of TUNEL and immunohistochemistry were categorized into five levels: -, no detection; ±, faint; +, weak; ++, moderate; +++, strong. The values show mean ± standard deviation. Data are mean ± standard deviation.

Histone acetylation and deacetylation are known to be regulated by Histone Acetyltransferases (HAT) and Histone Deacetylase (HDAC), respectively [1,2]. HDAC and HAT activities have been reported to be altered in liver damage, resulting in altered histone H3 and H4 acetylation levels [31]. Recently, loss of HDAC induced by treatment with DHAC inhibitors was reported to alter histone acetylation levels in the liver, resulting in significant delays in regenerative activities in the injured livers [8,9,32]. Thus, histone H4 acetylation plays an important role in liver regeneration after damage. Previous studies evaluated acetylation levels in whole liver tissues, but not cell-specific or zonal expression. Investigating the influence of histone deacetylation on liver regeneration in a cell-specific manner may aid in a better understanding of the pathobiological significance of histone acetylation in liver injury.

Conclusion

This study revealed the zone- and cell-specific distributions of acetylated H4 in normal mouse livers and the changes in acetylated H4 after initiation of acute liver injury with APAP. Most notably, histone acetylation in the hepatocytes of APAP-damaged livers underwent time-specific changes that correlated with tissue damage. Since a small number of animals were used, further work clarifying the mechanism(s) underlying epigenetic modifications in liver injury is warranted.

Acknowledgement

The authors thank Dr. Donna L. Mendrick, Dr. Richard D. Beger, Dr. Deborah K. Hansen, and Dr. Xuan Zhang for their useful suggestions. We also thank Dr. Kelly Davis for helping with the histological scoring and Ms. Lisa D. Freeman for helping to prepare the paraffin sections. The author (N.N) thanks Mr. Larry Schmued and Mr. Bryan Raymick for helping to capture the images.

This study was funded in part by the National Center for Toxicological Research (NCTR) (E0755202); liver paraffin blocks were also funded by the National Center for Toxicological Research (NCTR) (E07379.04).

Disclaimer: The views expressed are those of the authors and do not represent the views of the Food and Drug Administration.

References

1. Bird A. DNA methylation patterns and epigenetic memory. Genes Dev. 2002; 16: 6-21.
2. Eberharter A, Becker PB. Histone acetylation: a switch between repressive and permissive chromatin. Second in review series on chromatin dynamics. EMBO Rep. 2002; 3: 224-229.
3. Fischle W, Wang Y, Allis CD. Histone and chromatin cross-talk. Curr Opin Cell Biol. 2003; 15: 172-183.
4. Richardson BC. Role of DNA methylation in the regulation of cell function: autoimmunity, aging and cancer. J Nutr. 2002; 132: 2401-2405.

5. Baccarelli A, Ghosh S. Environmental exposures, epigenetics and cardiovascular disease. Curr Opin Clin Nutr Metab Care. 2012; 15: 323-329.

6. Gokul G, Khosla S. DNA methylation and cancer. Subcell Biochem. 2013; 61: 597-625.

7. Picascia A, Grimaldi V, Pignalosa O, De Pascale MR, Schiano C, Napoli C. Epigenetic control of autoimmune diseases: from bench to bedside. Clin Immunol. 2015; 157: 1-15.

8. Murata K, Hamada M, Sugimoto K, Nakano T. A novel mechanism for drug-induced liver failure: inhibition of histone acetylation by hydralazine derivatives. J Hepatol. 2007; 46: 322-329.

9. Ke Q, Yang RN, Ye F, Wang YJ, Wu Q, Li L, et al. Impairment of liver regeneration by the histone deacetylase inhibitor valproic acid in mice. J Zhejiang Univ Sci B. 2012; 13: 695-706.

10. Jungermann K, Kietzmann T. Zonation of parenchymal and nonparenchymal metabolism in liver. Annu Rev Nutr. 1996; 16: 179-203.

11. Yang X, Greenhaw J, Ali A, Shi Q, Roberts DW, Hinson JA, et al. Changes in mouse liver protein glutathionylation after acetaminophen exposure. J Pharmacol Exp Ther. 2012; 340: 360-368.

12. James LP, Mayeux PR, Hinson JA. Acetaminophen-induced hepatotoxicity. Drug Metab Dispos. 2003; 31: 1499-1506.

13. Kon K, Kim JS, Jaeschke H, Lemasters JJ. Mitochondrial permeability transition in acetaminophen-induced necrosis and apoptosis of cultured mouse hepatocytes. Hepatology. 2004; 40; 1170-1179.

14. McGill MR, Jaeschke H. Mechanistic biomarkers in acetaminophen-induced hepatotoxicity and acute liver failure: from preclinical models to patients. Expert Opin Drug Metab Toxicol. 2014; 10: 1005-1017.

15. National Research Council. Guide for the care and use of laboratory animals. 8th edn. Washington, DC: National Academy Press. 2011.

16. Lawson JA, Fisher MA, Simmons CA, Farhood A, Jaeschke H. Inhibition of Fas receptor (CD95)-induced hepatic caspase activation and apoptosis by acetaminophen in mice. Toxicol Appl Pharmacol. 1999; 156: 179-186.

17. Derelanko MJ. The toxicologist's pocket handbook. 2nd edn. Informa Healthcare, New York: National Academy Press. 2008.

18. Wade MG, Kawata A, Williams A, Yauk C. Methoxyacetic acid-induced spermatocyte death is associated with histone hyperacetylation in rats. Biol Reprod. 2008; 78: 822-831.

19. Bouwens L, Baekeland M, De Zanger R, Wisse E. Quantitation, tissue distribution and proliferation kinetics of Kupffer cells in normal rat liver. Hepatology. 1986; 6: 718-722.

20. R Core Team. R: A language and environment for statistical computing. Vienna, Austria: R Foundation for Statistical Computing. 2011.

21. Rahman I, Gilmour PS, Jimenez LA, MacNee W. Oxidative stress and TNF-alpha induce histone acetylation and NF-kappaB/AP-1 activation in alveolar epithelial cells: potential mechanism in gene transcription in lung inflammation. Mol Cell Biochem. 2002; 234-235: 239-248.

22. Ono S, Oue N, Kuniyasu H, Suzuki T, Ito R, Matsusaki K, et al. Acetylated histone H4 is reduced in human gastric adenomas and carcinomas. J Exp Clin Cancer Res. 2002; 21: 377-382.

23. Colnot S, Perret C. Liver zonation. Monga SPS, editor. In: Molecular pathology of liver diseases. New York: Springer. 2011; 7-16.

24. Kang LI, Mars WM, Michalopoulos GK. Signals and cells involved in regulating liver regeneration. Cells. 2012; 1: 1261-1292.

25. Theise ND, Saxena R, Portmann BC, Thung SN, Yee H, Chiriboga L, et al. The canals of Hering and hepatic stem cells in humans. Hepatology. 1999; 30: 1425-1433.

26. Zajicek G, Ariel I, Arber N. The streaming liver. III. Littoral cells accompany the streaming hepatocyte. Liver. 1988; 8: 213-218.

27. Salminen WF Jr, Voellmy R, Roberts SM. Differential heat shock protein induction by acetaminophen and a nonhepatotoxic regioisomer, 3'-hydroxyacetanilide, in mouse liver. J Pharmacol Exp Ther. 1997; 282: 1533-1540.

28. Zimmermann KC, Waterhouse NJ, Goldstein JC, Schuler M, Green DR. Aspirin induces apoptosis through release of cytochrome c from mitochondria. Neoplasia. 2000; 2: 505-513.

29. DeLeve LD. Liver sinusoidal endothelial cells and liver regeneration. J Clin Invest. 2013; 123: 1861-1866.

30. Bataller R, Brenner DA. Liver fibrosis. J Clin Invest. 2005; 115: 209-218.

31. Miura K, Taura K, Kodama Y, Schnabl B, Brenner DA. Hepatitis C virus-induced oxidative stress suppresses hepcidin expression through increased histone deacetylase activity. Hepatology. 2008; 48: 1420-1429.

32. Xia J, Zhou Y, Ji H, Wang Y, Wu Q, Bao J, et al. Loss of histone deacetylases 1 and 2 in hepatocytes impairs murine liver regeneration through Ki67 depletion. Hepatology. 2013; 58: 2089-2098.

Citation: Nakamura N, Chang C-W, Yang X, Shi Q, Salminen WF and Suzuki A. Distribution of Acetylated Histone 4 in Normal Liver and Acetaminophen-Induced Liver Damage. SM J Biol. 2017; 3(1): 1014.